Polynomial Chaos for Dispersive Electromagnetics

N. L. Gibson *
Department of Mathematics
Oregon State University

September 4, 2013

Abstract

Electromagnetic wave propagation in complex dispersive media is governed by the time dependent Maxwell's equations coupled to equations that describe the evolution of the induced macroscopic polarization. We consider "polydispersive" materials represented by distributions of dielectric parameters in a polarization model. The work focuses on a novel computational framework for such problems involving Polynomial Chaos Expansions as a method to improve the modeling accuracy of the Debye model and allow for easy simulation using the Finite Difference Time Domain (FDTD) method. Stability and dispersion analyzes are performed for the approach utilizing the second order Yee scheme in two spatial dimensions.

Keywords: Maxwell's equations; Debye polarization; relaxation time distribution; FDTD

1 Introduction

A fundamental question in electromagnetics is how to model dispersion and dissipation of the fields in complex materials such as biological tissue. This has most often led to the use of Maxwell's equations coupled with constitutive relationships for polarization. The problem is even more difficult with noisy data or variability (heterogeneity) in the material being interrogated. Some deterministic models have been generalized to an extent that they seem to account for this variability, but there is some question as to whether the resulting models are even physically realistic.

A recently rediscovered modeling framework allows uncertainty at the molecular level through distributions of parameters representing molecular variability. Intensive experimental efforts have been pursued in describing data for complex materials in the frequency domain with distributions of dielectric parameters, especially relaxation times in multiple Debye models. A significant amount of this work is reviewed in the survey paper by Foster and Schwan [24]. The corresponding time-domain inverse problems were initially developed in [5] and examples for a one dimensional case were solved in [6] using finite elements for the forward simulation and quadrature for computing the expected value over a distribution. Our contribution here is to describe an approximation approach, which utilizes the generalized Polynomial Chaos framework, in two and three dimensions. This allows the efficient use of the finite difference time domain (FDTD) method for solving the dispersive Maxwell's Equations, eliminates the need for a separate computation of expected values, and simplifies analysis of the model and numerical methods. The resulting approach can be applied to realistic two and three dimensional models of human tissue or geological media in an electromagnetic interrogation inverse problem.

*gibsonn@math.oregonstate.edu

1.1 Background

Ultra-short pulsed electromagnetic fields are used in a wide variety of applications such as radar, environmental and medical imaging to evaluate the internal structure of objects for detecting and characterizing anomalies. This is done by studying changes in the dielectric properties (such as permittivity, conductivity, and relaxation times) of the materials under consideration for example in the noninvasive evaluation of tissues and organs in cancer detection, and nondestructive investigation of materials for cracks. Time domain numerical simulations of wave propagation in dispersive materials can help in understanding the short-pulse response of these media, and can be used to obtain threshold levels of safe exposure of humans to high energy electromagnetic fields. These simulations can also be used in inverse problem formulations for natural resource exploration, among other applications. Thus, the numerical and computational analyses of such systems can provide great benefit in real world applications.

Microwave imaging for breast cancer detection has been considered in a numerical context by several researchers (c.f., [22, 49, 50] and references therein) due to the enhanced contrast that can be extracted through numerical inverse problem formulations over signal processing approaches. Likewise, there is active interest in microwave and other frequency remote sensing of the environment for accurate modeling (e.g., of ocean currents), or resource exploration (c.f., [21, 41] and references therein).

The detection, reconstruction, and characterization of objects in dielectrics using electromagnetic interrogation has been the subject of intense research for at least the past two decades. Numerical approaches generally fall into two categories: frequency-domain and time-domain.

We consider here broadband pulse (c.f., [64]) interrogation so as to excite multiple poles in the dielectric targets and to better distinguish between materials of interest. The use of multiple frequencies prohibits effective use of frequency domain methods, thus time domain approaches will be considered in modeling the interrogation problem. We note that frequency domain inverse problems may still be helpful in providing a baseline or initial approximation in an iterative inverse problem formulation.

In the context of time-domain forward simulations, the two most popular approaches are finite element method (FEM) [45, 52] and finite difference method (FD) [53, 54]. While FEM has advantages for characterizing complex domains, the cost of rebuilding the mesh and solving an implicit system at each iteration of the inverse problem is prohibitive. For this, and other reasons described below, we consider only finite difference methods in this work.

Additionally, most of the work done on inverse scattering and material characterization has been done for non-dispersive dielectrics, implying non-frequency dependent speed of propagation and attenuation. That is not to say that significant effort has not been put forth for forward simulation of dispersive dielectrics (c.f., [1, 3, 7, 47, 51, 8, 40, 37] among many others). Inverse problems for dispersive media are currently less prevalent [10, 59, 25, 4].

Considering the above, we will examine finite difference time domain (FDTD) methods [62, 46] for dispersive media [32, 35, 34, 63]. While numerical simulation methods have been developed for polydispersive (multiple pole) media such as biological tissue and wet soil, these methods are based on heuristic models with limited physical justification. For example the Cole-Cole model [19, 48] is known to accurately describe the dielectric response of a dispersive material over a wide range of frequencies. The model, however, does not lend itself easily to time domain simulation methods such as the Finite Difference Time Domain (FDTD) method or the Finite Element Method (FEM) (although attempts exist, c.f., [17, 39], however these are complicated to implement). Instead the physics-based Debye model (of which the Cole-Cole model is a non-physical, heuristic generalization) is often used. However, simulations do not match data over any broad range of

frequencies.

In this work, we seek to avoid the difficulty of implementing the Cole-Cole model by presenting a representation of dispersive mechanisms using distributions of parameters within the Debye model [2]. Empirical measurements suggest a log-normal or Beta distribution [16]. We modify the standard FDTD scheme to allow for distributions of dielectric parameters in a polarization model, and approximate the solution by using the Polynomial Chaos Expansion method.

We note that distributions of parameters in Maxwell's equations has been treated with Polynomial Chaos in [18], but this was not in the context of dispersive materials. The authors assumed unknown parameters which resulted in random solutions to Maxwell's equations. The current effort utilizes randomness as a modeling approach and results in a deterministic solution to Maxwell's equations.

2 Maxwell-Debye Model

In this section we review the necessary details of Maxwell's equations, which model the time propagation of electromagnetic fields, and polarization models (including Debye), which describe the material response to the fields. An energy decay property of the Maxwell-Debye Model is given.

2.1 Maxwell's Equations

We begin by introducing Maxwell's equations which govern the electric field $\mathbf{E}$ and the magnetic field $\mathbf{H}$ in a domain $\mathcal{D}$ with charge density ρ (which we take to be zero). Thus we first consider the system

$$\frac{\partial \mathbf{B}}{\partial t} + \nabla \times \mathbf{E} = 0, \text{ in } (0,T) \times \mathcal{D}, \tag{1a}$$

$$\frac{\partial \mathbf{D}}{\partial t} + \mathbf{J} - \nabla \times \mathbf{H} = 0, \text{ in } (0,T) \times \mathcal{D}, \tag{1b}$$

$$\nabla \cdot \mathbf{B} = 0, \text{ in } (0,T) \times \mathcal{D}, \tag{1c}$$

$$\nabla \cdot \mathbf{D} = \rho, \text{ in } (0,T) \times \mathcal{D}, \tag{1d}$$

$$\mathbf{E} \times \mathbf{n} = 0, \text{ on } (0,T) \times \partial\mathcal{D}, \tag{1e}$$

$$\mathbf{E}(0,\mathbf{x}) = 0, \quad \mathbf{H}(0,\mathbf{x}) = 0, \text{ in } \mathcal{D}. \tag{1f}$$

The current $\mathbf{J}$ is composed of the source current $\mathbf{J}_s$ and the conductive current $\mathbf{J}_c$. Initial conditions are specified in (1f), while Perfect Electrically Conducting (PEC) boundary conditions are imposed in (1e). Within the domain we have constitutive relations that relate the flux densities $\mathbf{D}$, $\mathbf{B}$ and the conductive current $\mathbf{J}_c$ to the electric and magnetic fields $\mathbf{E}$ and $\mathbf{H}$.

The Constitutive Laws describe the response of the medium to the electromagnetic field, including effects from polarization. These may assume the form

$$\mathbf{D} = \epsilon_0 \epsilon_\infty \mathbf{E} + \mathbf{P}, \tag{2a}$$

$$\mathbf{B} = \mu \mathbf{H} + \mathbf{M}, \tag{2b}$$

$$\mathbf{J} = \sigma \mathbf{E} + \mathbf{J}_s, \tag{2c}$$

where $\epsilon = \epsilon_0 \epsilon_\infty$. In (2), $\mathbf{D}$ and $\mathbf{E}$ represent the electric flux density and the electric field, respectively; $\mathbf{P}$ refers to the macroscopic polarization, $\mathbf{M}$ the magnetization, and $\mathbf{J}_s$ the source current

density. The dielectric parameters are ϵ_0, the electric permittivity of free space, ϵ_∞, the relative electric permittivity in the limit of infinite frequencies, μ, the magnetic permeability, and σ is the electric conductivity (which we take to be zero for simplicity).

Combining equations (1a) and (2b) under the assumptions that there is no magnetization and that $\mu = \mu_0$ (i.e., free space permeability) gives,

$$\mu_0 \frac{\partial \mathbf{H}}{\partial t} = -\nabla \times \mathbf{E}. \tag{3}$$

By combining equations (1b), (2a) and (2c) while neglecting the source term for simplicity we get,

$$\epsilon_0 \epsilon_\infty \frac{\partial \mathbf{E}}{\partial t} = -\sigma \mathbf{E} - \frac{\partial \mathbf{P}}{\partial t} + \nabla \times \mathbf{H}. \tag{4}$$

2.2 Polarization Models

Our main focus in this presentation is the dielectric polarization $\mathbf{P}$ which we assume has the general convolution form

$$\mathbf{P}(t, \mathbf{x}) = g \star \mathbf{E}(t, \mathbf{x}) = \int_0^t g(t - s, \mathbf{x}; \mathbf{q}) \mathbf{E}(s, \mathbf{x}) ds, \tag{5}$$

where g is the general dielectric response function (DRF), which can be thought of as representing the memory effect caused by the dielectric. In every practical example (Debye, Lorentz, etc.) DRFs are parameter dependent as well as time (and possibly space) dependent; we represent this as $g = g(t, \mathbf{x}; \mathbf{q})$, where typically $\mathbf{q}$ contains parameters such as the high frequency limit dielectric permittivity ϵ_∞, the static permittivity ϵ_s, and relaxation time τ. Examples of often-used DRFs are the Debye [4, 16, 20] defined in the time domain by

$$g(t, \mathbf{x}) = \epsilon_0(\epsilon_s - \epsilon_\infty)/\tau \;\; e^{-t/\tau}, \tag{6}$$

the Lorentz [4, 16, 33] given by

$$g(t, \mathbf{x}) = \epsilon_0 \omega_p^2 e^{-t/2\tau} \sin(\nu_0 t)/\nu_0,$$

and the Cole-Cole [16, 19, 26, 31, 48] defined by

$$g(t, \mathbf{x}) = \mathcal{L}^{-1} \left\{ \frac{\epsilon_0(\epsilon_s - \epsilon_\infty)}{1 + (s\tau)^\alpha} \right\} = \frac{1}{2\pi i} \int_{\zeta - i\infty}^{\zeta + i\infty} \frac{\epsilon_0(\epsilon_s - \epsilon_\infty)}{1 + (s\tau)^\alpha} e^{st} ds,$$

where $\mathcal{L}$ is the Laplace transform.

Substituting equation (5) into equation (2a) and taking the Laplace transform in time we get,

$$\hat{\mathbf{D}} = \epsilon(\omega) \hat{\mathbf{E}} \tag{7}$$

where ω is the angular frequency and $\epsilon(\omega)$ is the complex permittivity, which for the Debye model becomes,

$$\epsilon(\omega) = \epsilon_\infty + \frac{\epsilon_s - \epsilon_\infty}{1 + \mathrm{i}\omega\tau}. \tag{8}$$

The polarization in (5) defined by the Debye model (6) can be shown to be equivalent to the solution of the ordinary differential equation (ODE),

$$\tau \frac{\partial \mathbf{P}}{\partial t} + \mathbf{P} = \epsilon_0 \epsilon_d \mathbf{E}, \tag{9}$$

where $\epsilon_d = \epsilon_s - \epsilon_\infty$. The Lorentz model corresponds to a second order ODE, while the Cole-Cole model corresponds to the solution of a fractional order ODE model, the simulations of which are not straight-forward. We refer to equations (3) and (4) coupled with (9) as the Maxwell-Debye model.

The above models implicitly assume that single parameter values are representative of the dielectric response of materials. More realistically these parameters should be modeled as random variables with probability distributions, which we explore below. We note that the Cole-Cole model can be thought of as an approximation to the Debye model with a distribution of relaxation times, as can be seen through a Mellin transform of the Debye complex permittivity [16].

2.3 2D TE Maxwell-Debye Model

For simplicity in exposition and to facilitate analysis, we reduce the Maxwell-Debye model to two spatial dimensions. We emphasize that the methods described below apply in a straight-forward manner to the full three dimensional system.

To construct the 2D Transverse Electric (TE) Maxwell-Debye model we make the assumption that no fields exhibit variation in the z direction, i.e., all partial derivatives with respect to z are zero. The electric field and polarization each have two components, $\mathbf{E} = (E_x, E_y)^T, \mathbf{P} = (P_x, P_y)^T$ and the magnetic field has one component $H_z = H$. Combining (9) with (3) and (4), and reducing to two dimensions, we get the following three partial differential equations which we call the *2D Maxwell-Debye TE curl equations*:

$$\frac{\partial H}{\partial t} = -\frac{1}{\mu_0} \text{ curl } \mathbf{E}, \tag{10a}$$

$$\epsilon_0 \epsilon_\infty \frac{\partial \mathbf{E}}{\partial t} = \mathbf{curl}\ H - \frac{\epsilon_0 \epsilon_d}{\tau}\mathbf{E} + \frac{1}{\tau}\mathbf{P}, \tag{10b}$$

$$\frac{\partial \mathbf{P}}{\partial t} = \frac{\epsilon_0 \epsilon_d}{\tau}\mathbf{E} - \frac{1}{\tau}\mathbf{P}, \tag{10c}$$

where for a vector field, $\mathbf{U} = (U_x, U_y)^T$, the scalar curl operator is curl $\mathbf{U} = \frac{\partial U_y}{\partial x} - \frac{\partial U_x}{\partial y}$, and for a scalar field, V, the vector curl operator is $\mathbf{curl}\ V = \left(\frac{\partial V}{\partial y}, -\frac{\partial V}{\partial x}\right)^T$ [44]. All the fields in (10) are functions of position $\mathbf{x} = (x, y)^T$ and time t.

The system (10) along with the PEC boundary conditions and initial conditions $\mathbf{E}(\mathbf{x}, 0) = \mathbf{E}_0(\mathbf{x})$, $\mathbf{P}(\mathbf{x}, 0) = \mathbf{P}_0(\mathbf{x})$ and $H(\mathbf{x}, 0) = H_0(\mathbf{x})$ for $\mathbf{x} \in \mathcal{D} \subset \mathbb{R}^2$ was shown to be well-posed [14]. We recall the important results here for completeness and comparison to the analysis of our proposed approach. To this end, we define the following two function spaces:

$$H(\text{curl}, \mathcal{D}) = \{\mathbf{u} \in \left(L^2(\mathcal{D})\right)^2 ; \text{curl } \mathbf{u} \in L^2(\mathcal{D})\}, \tag{11}$$

$$H_0(\text{curl}, \mathcal{D}) = \{\mathbf{u} \in H(\text{curl}, \mathcal{D}), \mathbf{n} \times \mathbf{u} = 0\}. \tag{12}$$

Let $(\cdot, \cdot)_2$ denote the L^2 inner product and $||\cdot||_2$ the corresponding norm. Multiplying (10a) by $v \in L^2(\mathcal{D})$, (10b) by $\mathbf{u} \in H_0(\text{curl}, \mathcal{D})$, and (10c) by $\mathbf{w} \in \left(L^2(\mathcal{D})\right)^2$, integrating over the domain $\mathcal{D}$ and applying Green's formula for the **curl** operator

$$(\mathbf{curl}\ H, \mathbf{u}) = (H, \text{curl } \mathbf{u}), \ \forall \mathbf{u} \in H_0(\text{curl}, \mathcal{D}), \tag{13}$$

we obtain the weak formulation

$$\left(\frac{\partial H}{\partial t}, v\right)_2 = \left(-\frac{1}{\mu_0}\text{curl } \mathbf{E}, v\right)_2, \tag{14a}$$

$$\left(\epsilon_0\epsilon_\infty \frac{\partial \mathbf{E}}{\partial t}, \mathbf{u}\right)_2 = (H, \text{curl } \mathbf{u})_2 - \left(\frac{\epsilon_0\epsilon_d}{\tau}\mathbf{E}, \mathbf{u}\right)_2 + \left(\frac{1}{\tau}\mathbf{P}, \mathbf{u}\right)_2, \tag{14b}$$

$$\left(\frac{\partial \mathbf{P}}{\partial t}, \mathbf{w}\right)_2 = \left(\frac{\epsilon_0\epsilon_d}{\tau}\mathbf{E}, \mathbf{w}\right)_2 - \left(\frac{1}{\tau}\mathbf{P}, \mathbf{w}\right)_2. \tag{14c}$$

The following theorem shows the stability of the 2D TE Maxwell-Debye model (10) by showing that the model exhibits energy decay [38].

Theorem 2.1. *Let $\mathcal{D} \subset \mathbb{R}^2$ and suppose that $\mathbf{E} \in C(0,T; H_0(\text{curl}, \mathcal{D})) \cap C^1(0,T; (L^2(\mathcal{D}))^2)$, $\mathbf{P} \in C^1(0,T; \left(L^2(\mathcal{D})\right)^2)$, and $H(t) \in C^1(0,T; L^2(\mathcal{D}))$ are solutions of the weak formulation (14) for the Maxwell-Debye system of equations (10) along with PEC boundary conditions. Then the system exhibits energy decay,*

$$\mathcal{E}(t) \leq \mathcal{E}(0) \quad \forall t \geq 0, \tag{15}$$

where the energy $\mathcal{E}(t)$ is defined as

$$\mathcal{E}(t) = \left(\left\| \sqrt{\mu_0}\ H(t) \right\|_2^2 + \left\| \sqrt{\epsilon_0\epsilon_\infty}\ \mathbf{E}(t) \right\|_2^2 + \left\| \frac{1}{\sqrt{\epsilon_0\epsilon_d}}\ \mathbf{P}(t) \right\|_2^2 \right)^{\frac{1}{2}}. \tag{16}$$

In [38], it is also shown that the Gauss laws (1c), (1d) are satisfied by the Maxwell-Debye system if the initial fields are divergence free.

3 Maxwell-Random Debye

The macroscopic polarization model (5) can be derived from microscopic dipole, electron cloud, etc., formulations by passing to a limit over the molecular population. However, such derivations tacitly assume that one has similar individual (molecular, dipole, etc.) parameters; that is, all dipoles, molecules, "electron clouds", etc., have the same relaxation parameters, plasma frequencies, etc. Historically, such models based on molecular level homogeneity throughout the material have often not performed well when trying to compare models with experimental data. Indeed, in 1907 Von Schweidler [16, 57] observed the need to assume *multiple relaxation times* when considering experimental data and in 1913 Wagner [16, 58] proposed continuous distributions of relaxation times.

In the past half century intensive experimental efforts [23, 26, 27, 28, 29, 31, 43] have been pursued in describing data for complex materials with distributions of dielectric parameters (especially relaxation times in multiple Debye [23] or multiple Lorentz [33] mechanisms) in the frequency domain. A significant amount of this work is reviewed in the survey paper by Foster and Schwan [23]. There are now *incontrovertible* experimentally based arguments for distributions of relaxation parameters in mechanisms for heterogeneous materials.

3.1 Maxwell-Random Debye Model Formulation

We may assume that the dielectric parameters ϵ_∞ and ϵ_s are constant and known. The usual Debye model presumes that the material may be sufficiently defined by a single relaxation parameter τ,

which is generally not the case. In order to account for uncertainty in the polarization mechanisms, we allow for a distribution of relaxation parameters, and subsequently refer to these types of materials as *polydispersive*. Thus, we define our polarization model in terms of a distribution-dependent dielectric response function h

$$\mathbf{P}(t,\mathbf{x};F) = \int_0^t h(t-s,\mathbf{x};F)\mathbf{E}(s,\mathbf{x})ds, \tag{17}$$

where h is determined by a family of polarization laws each described by a different parameter τ, and therefore is given by

$$h(t,\mathbf{x};F) = \int_\Omega g(t,\mathbf{x};\tau)dF(\tau),$$

where $\Omega = [\tau_a, \tau_b] \subset (0,\infty)$. In particular, if the distribution F were discrete, consisting of a single relaxation parameter, then we would again have (9). In the case when τ has a uniform distribution, $dF(\tau) = f(\tau)d\tau$ with

$$f(\tau) = \frac{1}{\tau_b - \tau_a}.$$

The macroscopic electric polarization becomes

$$\mathbf{P}(t,\mathbf{x}) = \int_0^t \left[\int_\Omega g(t-s,\mathbf{x};\tau)dF(\tau)\right]\mathbf{E}(s,\mathbf{x})ds,$$

or, interchanging integrals, we have

$$\mathbf{P}(t,\mathbf{x}) = \int_\Omega \mathcal{P}(t,\mathbf{x};\tau)dF(\tau) = \mathbb{E}[\mathcal{P}], \tag{18}$$

where

$$\mathcal{P}(t,\mathbf{x};\tau) = \int_0^t g(t-s,\mathbf{x};\tau)\mathbf{E}(s,\mathbf{x})ds$$

is the *random polarization* due to the *random relaxation parameter* τ. The random polarization is the microscopically chaotic polarization that is influenced by distributions of τ. We take the macroscopic polarization, which appears in Maxwell's equations via the constitutive laws, to be the expected value of the random polarization. In the case of the Debye model, the random polarization can be expressed as the solution to a first order *random ordinary differential equation* (RODE) where the relaxation time τ is modeled as a random variable

$$\tau\frac{\partial\mathcal{P}}{\partial t} + \mathcal{P} = \epsilon_0\epsilon_d\mathbf{E}. \tag{19}$$

Remark 3.1. *Existence and uniqueness of solutions to a weak formulation of the 1D version of the Maxwell-Random Debye problem, as well as continuous dependence of $(E,\dot{E})$ on F in the Prohorov metric was shown in [5].*

Remark 3.2. *A bi-modal (mixture distribution) model may be derived in a similar fashion. This is the random analog to multi-pole Debye models. Consider that the polarization is driven by two distinct mechanisms, one with a dielectric distribution determined by mean μ_1 and standard deviation σ_1, and the other determined by mean μ_2 and standard deviation σ_2. Then we may define $F_1(\tau;\mu_1,\sigma_1)$ and $F_2(\tau;\mu_2,\sigma_2)$ as distributions and let our macroscopic electric polarization be a function of some combination of these distributions (e.g., determined by the relative volume percentage of each of two substances in a material). Thus if $dF(\tau) = \beta_1 dF_1(\tau) + \beta_2 dF_2(\tau)$ then we again have the representation* (18).

Remark 3.3 (Distribution Parameter Fit to Data)**.** *When random dielectric parameters are assumed in the Maxwell system, the result is a system of partial differential equations where the solutions depend on probability measures. These measures are now the "parameters" that characterize the material dielectric properties which one must estimate with data or identify in interrogation problems.*

One may use an inverse problem formulation (e.g., non-linear least squares method) to determine the correct distribution of τ. This has been done in the time domain using direct simulation of the Maxwell-Random Debye model [6] and via Induced Polarization [55].

More commonly, the distribution parameters are fit in the frequency domain using complex permittivity measurements. The most popular of these approaches is the multi-pole Debye model [31, 36], which is even used to approximate non-Debye poles due to the simplicity of the forward simulation of the Maxwell-Debye model. (We note that while many materials exhibit multiple polarization mechanisms and therefore have distinct relaxation poles, the multi-pole approach is commonly used to approximate single poles, in which case we understand these to be discrete distribution approximations to a true continuous distribution of parameters.) Other approaches include non-parametric [12], a parameterized Cole-Cole distribution [56], and a parameterized uniform Random Debye model [9]. In the latter, the uniform Debye was shown to be nearly as accurate as the single Cole-Cole model for dry skin permittivity data [26], which is significant in that the Cole-Cole model is difficult to simulate [17].

In a polydisperse Debye material, we then have the following Maxwell-Random Debye problem: find $\mathbf{E}, \mathbf{H}, \mathcal{P}$ with $E_w \in C(0,T;H_0(\text{curl},\mathcal{D})) \cap\ C^1(0,T;L^2(\mathcal{D}))$, $H \in C^1(0,T;L^2(\mathcal{D}))$, and $\mathcal{P}_w \in C^1(0,T;L^2(\Omega)\otimes L^2(\mathcal{D}))$, for each spatial component $w = \{x, y\}$, such that F-almost everywhere in Ω (or almost surely), the following equations (*2D TE Maxwell-Random Debye*) model hold

$$\frac{\partial H}{\partial t} = -\frac{1}{\mu_0}\ \text{curl}\ \mathbf{E}, \tag{20a}$$

$$\epsilon_0\epsilon_\infty \frac{\partial \mathbf{E}}{\partial t} = \mathbf{curl}\ H - \frac{\partial \mathbf{P}}{\partial t}, \tag{20b}$$

$$\tau\frac{\partial \mathcal{P}}{\partial t} + \mathcal{P} = \epsilon_0\epsilon_d\mathbf{E}, \tag{20c}$$

along with (18).

For ease of notation, we introduce the Hilbert space $V_F = (L^2(\Omega))^2 \otimes (L^2(\mathcal{D}))^2$ equipped with an inner product and norm as follows

$$(u,v)_F = \mathbb{E}[(u,v)_2],$$
$$\|u\|_F^2 = \mathbb{E}[\|u\|_2^2].$$

3.2 Stability Result

The following theorem shows the stability of the 2D TE Maxwell-Random Debye model, (20) along with (18), by showing that the model exhibits energy decay. The weak formulation consists of equations (14a) along with

$$\left(\epsilon_0\epsilon_\infty\frac{\partial \mathbf{E}}{\partial t}, \mathbf{u}\right)_2 = (H, \text{curl}\ \mathbf{u})_2 - \left(\frac{\partial \mathbf{P}}{\partial t}, \mathbf{u}\right)_2, \tag{21}$$

$$\left(\frac{\partial \mathcal{P}}{\partial t}, \mathbf{w}\right)_F = \left(\frac{\epsilon_0\epsilon_d}{\tau}\mathbf{E}, \mathbf{w}\right)_F - \left(\frac{1}{\tau}\mathcal{P}, \mathbf{w}\right)_F \tag{22}$$

for $\mathbf{u} \in H_0(\text{curl},\mathcal{D})$ and $\mathbf{w} \in V_F^2$.

Theorem 3.1 (Energy Decay for the Maxwell-Random Debye System)**.** *Let $\mathcal{D} \subset \mathbb{R}^2$ and suppose that $\mathbf{E} \in C(0,T;H_0(\text{curl},\mathcal{D})) \cap C^1(0,T;(L^2(\mathcal{D}))^2)$, $\mathcal{P} \in C^1(0,T;(V_F)^2)$, and $H \in C^1(0,T;L^2(\mathcal{D}))$ are solutions of the weak formulation for the 2D Maxwell-Random Debye system of equations* (14a)*,* (21) *and* (22) *along with PEC boundary conditions. Then the system exhibits energy decay,*

$$\mathcal{E}(t) \leq \mathcal{E}(0) \quad \forall t \geq 0, \tag{23}$$

where the energy $\mathcal{E}(t)$ is defined as

$$\mathcal{E}(t) = \left(\left\| \sqrt{\mu_0}\ H(t) \right\|_2^2 + \left\| \sqrt{\epsilon_0 \epsilon_\infty}\ \mathbf{E}(t) \right\|_2^2 + \left\| \frac{1}{\sqrt{\epsilon_0 \epsilon_d}}\ \mathcal{P}(t) \right\|_F^2 \right)^{\frac{1}{2}}. \tag{24}$$

Proof. The proof is straight-forward after replacing inner products in the proof of Theorem 2.1 [38] with $(\cdot,\cdot)_F$ and norms with $\|\cdot\|_F$. For completeness we show the details below.

By choosing $v = H,\ \mathbf{u} = \mathbf{E}$, and $\mathbf{w} = \mathcal{P}$ in (14a), (21) and (22), and adding all three equations into the time derivative of the definition of $\mathcal{E}^2$, we obtain

$$\begin{aligned}
\frac{1}{2}\frac{d\mathcal{E}^2(t)}{dt} =& -\Big(\text{curl }\mathbf{E}, H\Big)_2 + \Big(H, \text{curl }\mathbf{E}\Big)_2 - \Big(\frac{\partial \mathbf{P}}{\partial t}, \mathbf{E}\Big)_2 + \Big(\frac{1}{\tau}\mathbf{E}, \mathcal{P}\Big)_F - \Big(\frac{1}{\epsilon_0 \epsilon_d \tau}\mathcal{P}, \mathcal{P}\Big)_F \\
=& -\Big(\text{curl }\mathbf{E}, H\Big)_2 + \Big(H, \text{curl }\mathbf{E}\Big)_2 - \Big(\frac{\epsilon_0\epsilon_d}{\tau}\mathbf{E}, \mathbf{E}\Big)_F + \Big(\frac{1}{\tau}\mathcal{P}, \mathbf{E}\Big)_F \\
&+ \Big(\frac{1}{\tau}\mathbf{E}, \mathcal{P}\Big)_F - \Big(\frac{1}{\epsilon_0 \epsilon_d \tau}\mathcal{P}, \mathcal{P}\Big)_F \\
=& -\epsilon_0\epsilon_d\Big(\frac{1}{\tau}\mathbf{E}, \mathbf{E}\Big)_F + 2\Big(\frac{1}{\tau}\mathcal{P}, \mathbf{E}\Big)_F - \frac{1}{\epsilon_0\epsilon_d}\Big(\frac{1}{\tau}\mathcal{P}, \mathcal{P}\Big)_F \\
=& \frac{-1}{\epsilon_0\epsilon_d}\left\| \frac{1}{\tau}(\mathcal{P} - \epsilon_0\epsilon_d\mathbf{E}) \right\|_F^2.
\end{aligned}$$

Thus, we finally have

$$\frac{d\mathcal{E}^2(t)}{dt} = \frac{-2}{\epsilon_0\epsilon_d}\left\| \frac{1}{\tau}\left(\mathcal{P} - \epsilon_0\epsilon_d\mathbf{E}\right) \right\|_F^2 \leq 0. \tag{25}$$

In particular, we have

$$\frac{d\mathcal{E}(t)}{dt} = \frac{-1}{\epsilon_0\epsilon_d\mathcal{E}(t)}\left\| \frac{1}{\tau}\left(\mathcal{P} - \epsilon_0\epsilon_d\mathbf{E}\right) \right\|_F^2 \leq 0. \tag{26}$$

Therefore the energy, $\mathcal{E}(t)$, is decreasing and $\mathcal{E}(t) \leq \mathcal{E}(0)\ \forall t > 0$. ∎

3.3 Dispersion Relation

The following theorem gives the dispersion relation for the Maxwell-Random Debye model, which will be compared to the fully discretized version to determine any numerical dispersion error.

Theorem 3.2. *The exact* dispersion relation *for the system* (20) *is given by*

$$\frac{\omega^2}{c^2}\epsilon(\omega) = |\vec{k}|^2, \tag{27}$$

where the expected complex permittivity *is given by*

$$\epsilon(\omega) = \epsilon_\infty + \epsilon_d \mathbb{E}\left[\frac{1}{1 - \mathrm{i}\omega\tau}\right]. \tag{28}$$

Here, $\vec{k}$ is the wave number and $c = 1/\sqrt{\mu_0\epsilon_0}$ is the speed of light in free space. This is the same form as for the non-random Debye model in that the expectation in that case is the identity.

Proof. As the proof is similar in 1 and 3 dimensions, we describe only the 2D case here. Letting $H = H_z$, we have the *2D Maxwell-Random Debye TE* scalar equations:

$$\frac{\partial H}{\partial t} = \frac{1}{\mu_0}\left(\frac{\partial E_x}{\partial y} - \frac{\partial E_y}{\partial x}\right), \tag{29a}$$

$$\epsilon_0\epsilon_\infty \frac{\partial E_x}{\partial t} = \frac{\partial H}{\partial y} - \frac{\partial P_x}{\partial t}, \tag{29b}$$

$$\epsilon_0\epsilon_\infty \frac{\partial E_y}{\partial t} = -\frac{\partial H}{\partial x} - \frac{\partial P_y}{\partial t}, \tag{29c}$$

$$\tau\frac{\partial \mathcal{P}_x}{\partial t} + \mathcal{P}_x = \epsilon_0\epsilon_d E_x \tag{29d}$$

$$\tau\frac{\partial \mathcal{P}_y}{\partial t} + \mathcal{P}_y = \epsilon_0\epsilon_d E_y, \tag{29e}$$

along with (18).

We assume plane wave solutions of the form

$$V = \widetilde{V}\mathrm{e}^{\mathrm{i}(k_x x + k_y y - \omega t)},$$

and let $\vec{x} = (x, y)^T$ and $\vec{k} = (k_x, k_y)^T$. Then (29) becomes

$$-\mathrm{i}\omega\widetilde{H} = \frac{1}{\mu_0}\left(\mathrm{i}k_y\widetilde{E}_x - \mathrm{i}k_x\widetilde{E}_y\right), \tag{30a}$$

$$-\epsilon_0\epsilon_\infty\mathrm{i}\omega\widetilde{E}_x = \mathrm{i}k_y\widetilde{H} - (-\mathrm{i}\omega\widetilde{P}_x), \tag{30b}$$

$$-\epsilon_0\epsilon_\infty\mathrm{i}\omega\widetilde{E}_y = -\mathrm{i}k_x\widetilde{H} - (-\mathrm{i}\omega\widetilde{P}_y), \tag{30c}$$

$$-\mathrm{i}\omega\tau\widetilde{\mathcal{P}}_x + \widetilde{\mathcal{P}}_x = \epsilon_0\epsilon_d\widetilde{E}_x \tag{30d}$$

$$-\mathrm{i}\omega\tau\widetilde{\mathcal{P}}_y + \widetilde{\mathcal{P}}_y = \epsilon_0\epsilon_d\widetilde{E}_y. \tag{30e}$$

By (30d) we have

$$\widetilde{P}_x = \mathbb{E}[\widetilde{\mathcal{P}}_x] = \epsilon_0\epsilon_d\widetilde{E}_x\mathbb{E}\left[\frac{1}{1-\mathrm{i}\omega\tau}\right]. \tag{31}$$

Substituting into (30b) we have

$$\begin{aligned} -\epsilon_0\epsilon_\infty\mathrm{i}\omega\widetilde{E}_x &= \mathrm{i}k_y\widetilde{H} + \left(\mathrm{i}\omega\epsilon_0\epsilon_d\widetilde{E}_x\mathbb{E}\left[\frac{1}{1-\mathrm{i}\omega\tau}\right]\right), \\ -\mathrm{i}\omega\epsilon_0\left(\epsilon_\infty + \epsilon_d\mathbb{E}\left[\frac{1}{1-\mathrm{i}\omega\tau}\right]\right)\widetilde{E}_x &= \mathrm{i}k_y\widetilde{H}, \\ -\mathrm{i}\omega\epsilon_0\epsilon(\omega)\widetilde{E}_x &= \mathrm{i}k_y\widetilde{H}. \end{aligned} \tag{32}$$

In the above we have used the definition of the complex permittivity from (28). Similarly combining (30e) and (30c) gives

$$-\mathrm{i}\omega\epsilon_0\epsilon(\omega)\widetilde{E}_y = -\mathrm{i}k_x\widetilde{H}. \tag{33}$$

Substituting both (32) and (33) into (30a) yields

$$\begin{aligned} -\mathrm{i}\omega\widetilde{H} &= \frac{1}{\mu_0}\left(\frac{(\mathrm{i}k_y)^2}{-\mathrm{i}\omega\epsilon_0\epsilon(\omega)} + \frac{(\mathrm{i}k_x)^2}{-\mathrm{i}\omega\epsilon_0\epsilon(\omega)}\right)\widetilde{H}, \\ -(\mathrm{i}\omega)^2\mu_0\epsilon_0\epsilon(\omega) &= k_y^2 + k_x^2 \\ \frac{\omega^2}{c^2}\epsilon(\omega) &= |\vec{k}|^2. \end{aligned}$$

□

Remark 3.4. *In the case of a uniform distribution on $[\tau_a, \tau_b]$, the expected complex permittivity has an analytic form since*

$$\mathbb{E}\left[\frac{1}{1-\mathrm{i}\omega\tau}\right] = \frac{1}{(\tau_b-\tau_a)\omega}\left[\arctan(\omega\tau) - \mathrm{i}\frac{1}{2}\ln\left(1+(\omega\tau)^2\right)\right]_{\tau=\tau_a}^{\tau=\tau_b}.$$

4 Maxwell-PC Debye

Toward a solution to the Maxwell-Random Debye model, one needs an efficient method for the computation of the expected value of the random polarization. One could apply a quadrature rule to the integral in the expected value [6]. This approach results in a linear combination of individual Debye models, and is equivalent to the multi-pole Debye approximation [31]. Alternatively, we propose to use a spectral method in random space, called *polynomial chaos* (PC) [60, 61]. Polynomial chaos is a method for expressing stochastic solutions in terms of truncated expansions of orthogonal polynomials of the random inputs. The family of orthogonal polynomials is generally chosen to be orthogonal with respect to the probability measure corresponding to the random inputs. The popularity of the method is due to the potential for exponential convergence of the L_2 error in terms of the number of orthogonal polynomials required in the truncated expansion. The method is especially efficient for low random dimension.

The PC approach results in a deterministic, linear system of auxiliary ordinary differential equations (coupled to Maxwell's Equations) for an approximation to the random polarization given in (19). Specifically, in each spatial dimension ($E = \mathbf{E}_j$, for $j = x, y, z$) we have

$$\tau\dot{\mathcal{P}} + \mathcal{P} = \epsilon_0\epsilon_d E, \quad \tau = \tau(\xi) = \tau_r\xi + \tau_m,$$

where the relaxation time is modeled as a random variable with, e.g., $\xi \sim \mathrm{Beta}(a, b)$ or uniform on $[-1, 1]$, and where τ_m and τ_r are shift and scaling parameters, respectively. Then the PC system is (after a Galerkin projection onto the finite dimensional random space spanned by the first $p+1$ orthogonal polynomials)

$$(\tau_r\mathcal{M} + \tau_m I)\dot{\vec{\alpha}} + \vec{\alpha} = \epsilon_0\epsilon_d E\hat{e}_1$$

or

$$A\dot{\vec{\alpha}} + \vec{\alpha} = \vec{f}. \tag{34}$$

In the above,

$$\mathcal{M} = \begin{bmatrix} b_0 & a_1 & & & \\ c_0 & b_1 & a_2 & & \\ & \ddots & \ddots & \ddots & \\ & & \ddots & \ddots & a_p \\ & & & c_{p-1} & b_p \end{bmatrix},$$

where the diagonals come from the coefficients of the triple recursion formula for the choice of family of orthogonal polynomials [30]

$$\xi\phi_j = a_j\phi_{j-1} + b_j\phi_j + c_j\phi_{j+1}$$

(with the assumption that $\phi_{-1} \equiv 0$ and $\phi_0 \equiv 1$). The solution vector $\vec{\alpha} = [\alpha_0, \ldots, \alpha_p]^T$ represents the truncated expansion up to degree p of the random polarization in the basis of orthogonal polynomials

$$\mathcal{P}(t, x, \xi) = \sum_{i=0}^{\infty} \alpha_i(t, x)\phi_i(\xi). \tag{35}$$

See [11] for the details of the derivation.

Note that the deterministic value $\vec{f}$ forces the system and is dependent on the electric field governed by Maxwell's equations. Maxwell's equations are coupled to the macroscopic polarization, i.e., the expected value of the random polarization at each point (t, x), which is well approximated by

$$P(t, x; F) = \mathbb{E}[\mathcal{P}] \approx \alpha_0(t, x). \tag{36}$$

If the chosen set of orthogonal polynomials are orthogonal with respect to the density function of the random variable ξ, then the error in this approximation of the expected value converges exponentially with p (as we demonstrated in [11]). Thus the Maxwell-PC Debye model consists of replacing the RODE (19) in the Maxwell-Random Debye model with the deterministic system of ODEs (34) and making the approximation (36), for example, in two dimensions we have the *2D Maxwell-PC Debye TE* scalar equations

$$\frac{\partial H}{\partial t} = \frac{1}{\mu_0}\left(\frac{\partial E_x}{\partial y} - \frac{\partial E_y}{\partial x}\right), \tag{37a}$$

$$\epsilon_0\epsilon_\infty \frac{\partial E_x}{\partial t} = \frac{\partial H}{\partial y} - \frac{\partial \alpha_{0,x}}{\partial t}, \tag{37b}$$

$$\epsilon_0\epsilon_\infty \frac{\partial E_y}{\partial t} = -\frac{\partial H}{\partial x} - \frac{\partial \alpha_{0,y}}{\partial t}, \tag{37c}$$

$$A\dot{\vec{\alpha}}_x + \vec{\alpha}_x = \vec{f}_x, \tag{37d}$$

$$A\dot{\vec{\alpha}}_y + \vec{\alpha}_y = \vec{f}_y. \tag{37e}$$

We remark that for Beta random variables, Jacobi polynomials are used, and for uniform random variables, Legendre polynomials are used [61]. As an example, if we choose a uniform random variable, then for the case when $p = 2$ we obtain the following system for the PC Debye model:

$$A = \begin{pmatrix} \tau_m & \frac{1}{3}\tau_r & 0 \\ \tau_r & \tau_m & \frac{2}{5}\tau_r \\ 0 & \frac{2}{3}\tau_r & \tau_m \end{pmatrix}.$$

However, if $\xi \sim \text{Beta}(2, 5)$, and $p = 2$, then

$$A = \begin{pmatrix} \frac{1}{3}\tau_r + \tau_m & \frac{2}{5}\tau_r & 0 \\ \frac{2}{9}\tau_r & \frac{7}{33}\tau_r + \tau_m & \frac{14}{33}\tau_r \\ 0 & \frac{18}{55}\tau_r & \frac{21}{143}\tau_r + \tau_m \end{pmatrix}.$$

Clearly as $\tau_r \to 0$ then the PC Debye model converges to a diagonal, uncoupled Debye ODE with a single relaxation time of $\tau = \tau_m$, which can be thought of as modeled by a delta distribution.

Remark 4.1 (The Invertibility of A)**.** *In order to solve the PC system for $\dot{\vec{\alpha}}$ the matrix A must be non-singular. This is true as long as $\tau_r < \tau_m$ since the eigenvalues of $\mathcal{M}$ are in $(-1, 1)$ [30], and therefore the eigenvalues of A are greater than $\tau_m - \tau_r$, thus A is in fact positive definite.*

5 Maxwell-PC Debye-FDTD

We now describe a discretization of the Maxwell-PC Debye model. We note that any spatial or temporal discretization scheme could be used, independently of the spectral approach in random space employed here. The purpose in choosing an FDTD discretization is both for ease of comparison with the vast literature on FDTD methods, as well as for practical terms in that FDTD methods are extremely computationally efficient, even in three dimensions, while being simple to implement, and therefore most likely to be used by practitioners in actual simulations of polydispersive materials. We emphasize that the discretization of the Maxwell-PC Debye differs from a discretization of a Maxwell-Debye system only in the treatment of the auxiliary differential equation.

5.1 Discretization

Below we follow the setup described in [14] for the development of the Yee scheme for dispersive materials. Consider the spatial domain $\Omega = [0, a] \times [0, b] \subset \mathbb{R}^2$ and time interval $[0, T]$ with a, b, $T > 0$ and spatial step sizes $\Delta x > 0$ and $\Delta y > 0$ and time step $\Delta t > 0$. The discretization of the intervals $[0, a]$, $[0, b]$, and $[0, T]$ is performed as follows. Define $L = a/\Delta x$, $J = b/\Delta y$ and $N = T/\Delta t$. For $\ell, j, n \in \mathbb{N}$ we consider the discretizations

$$0 = x_0 \leq x_1 \leq \cdots \leq x_\ell \leq \cdots \leq x_L = a, \tag{38}$$

$$0 = y_0 \leq y_1 \leq \cdots \leq y_j \leq \cdots \leq y_J = b, \tag{39}$$

$$0 = t^0 \leq t^1 \leq \cdots \leq t^n \leq \cdots \leq t^N = T, \tag{40}$$

where $x_\ell = \ell \Delta x$, $y_j = j\Delta y$, and $t^n = n\Delta t$ for $0 \leq \ell \leq L$, $0 \leq j \leq J$, and $0 \leq n \leq N$. Define $(x_\alpha, y_\beta, t^\gamma) = (\alpha\Delta x, \beta\Delta y, \gamma\Delta t)$ where α is either ℓ or $\ell + \frac{1}{2}$, β is either j or $j + \frac{1}{2}$, and γ is either n or $n + \frac{1}{2}$ with $\ell, j, n \in \mathbb{N}$. The operator splitting schemes like the Yee scheme stagger the electric and magnetic fields in space. Fields E_x, E_y, and H are staggered in the x and y directions. We define the discrete meshes

$$\tau_h^{E_x} := \left\{ \left(x_{\ell+\frac{1}{2}}, y_j \right) | 0 \leq \ell \leq L-1, 0 \leq j \leq J \right\}, \tag{41}$$

$$\tau_h^{E_y} := \left\{ \left(x_\ell, y_{j+\frac{1}{2}} \right) | 0 \leq \ell \leq L, 0 \leq j \leq J-1 \right\}, \tag{42}$$

$$\tau_h^{H} := \left\{ \left(x_{\ell+\frac{1}{2}}, y_{j+\frac{1}{2}} \right) | 0 \leq \ell \leq L-1, 0 \leq j \leq J-1 \right\}, \tag{43}$$

to be the sets of spatial grid points on which the E_x, E_y, and H fields, respectively, will be discretized. The components P_x and P_y of the polarization are discretized at the same spatial locations as the fields E_x and E_y, respectively. For the time discretization, the components E_x, E_y, P_x, P_y are all discretized at integer time steps t^n for $0 \leq n \leq N$. In the Yee scheme, the magnetic field, H, is staggered in time with respect to E_x and E_y and discretized at $t^{n+\frac{1}{2}}$ for $0 \leq n \leq N-1$.

Let U be one of the field variables H, E_x, E_y, P_x or P_y, and $(x_\alpha, y_\beta) \in \tau_h^H, \tau_h^{E_x}$ or $\tau_h^{E_y}$, and γ be either n or $n + \frac{1}{2}$ with $\gamma \leq N$. We define the *grid functions* or the numerical approximations

$$U_{\alpha,\beta}^\gamma \approx U(x_\alpha, y_\beta, t^\gamma).$$

We will also use the notation $U(t^\gamma)$ to denote the continuous solution on the domain Ω at time t^γ, and the notation U^γ to denote the corresponding grid function on its discrete mesh at time t^γ.

We define the centered temporal difference operator and a discrete time averaging operation as

$$\delta_t U^\gamma_{\alpha,\beta} := \frac{U^{\gamma+\frac{1}{2}}_{\alpha,\beta} - U^{\gamma-\frac{1}{2}}_{\alpha,\beta}}{\Delta t}, \tag{44}$$

$$\overline{U}^\gamma_{\alpha,\beta} := \frac{U^{\gamma+\frac{1}{2}}_{\alpha,\beta} + U^{\gamma-\frac{1}{2}}_{\alpha,\beta}}{2}, \tag{45}$$

and the centered spatial difference operators in the x and y direction, respectively as

$$\delta_x U^\gamma_{\alpha,\beta} := \frac{U^\gamma_{\alpha+\frac{1}{2},\beta} - U^\gamma_{\alpha-\frac{1}{2},\beta}}{\Delta x}, \tag{46}$$

$$\delta_y U^\gamma_{\alpha,\beta} := \frac{U^\gamma_{\alpha,\beta+\frac{1}{2}} - U^\gamma_{\alpha,\beta-\frac{1}{2}}}{\Delta y}. \tag{47}$$

Next, we define the following staggered l^2 normed spaces

$$\mathbb{V}_H := \left\{ U : \tau_h^H \longrightarrow \mathbb{R} \mid U = (U_{l+\frac{1}{2},j+\frac{1}{2}}), \|\mathbf{U}\|_E < \infty \right\}, \tag{48}$$

$$\mathbb{V}_E := \left\{ \mathbf{F} : \tau_h^{E_x} \times \tau_h^{E_y} \longrightarrow \mathbb{R}^2 \mid \mathbf{F} = (F_{x_{l+\frac{1}{2},j}}, F_{y_{l,j+\frac{1}{2}}})^T, \|\mathbf{F}\|_E < \infty \right\}, \tag{49}$$

where the discrete L^2 grid norms are defined as

$$\|\mathbf{F}\|_E^2 = \Delta x \Delta y \sum_{\ell=0}^{L-1} \sum_{j=0}^{J-1} \left(|F_{x_{\ell+\frac{1}{2},j}}|^2 + |F_{y_{\ell,j+\frac{1}{2}}}|^2 \right), \forall\ \mathbf{F} \in \mathbb{V}_E, \tag{50}$$

$$\|U\|_H^2 = \Delta x \Delta y \sum_{\ell=0}^{L-1} \sum_{j=0}^{J-1} |U_{\ell+\frac{1}{2},j+\frac{1}{2}}|^2, \forall\ U \in \mathbb{V}_H, \tag{51}$$

with corresponding inner products

$$(\mathbf{F}, \mathbf{G})_E = \Delta x \Delta y \sum_{\ell=0}^{L-1} \sum_{j=0}^{J-1} \left(F_{x_{\ell+\frac{1}{2},j}} G_{x_{\ell+\frac{1}{2},j}} + F_{y_{\ell,j+\frac{1}{2}}} G_{y_{\ell,j+\frac{1}{2}}} \right), \forall\ \mathbf{F}, \mathbf{G} \in \mathbb{V}_E, \tag{52}$$

$$(U, V)_H = \Delta x \Delta y \sum_{\ell=0}^{L-1} \sum_{j=0}^{J-1} U_{\ell+\frac{1}{2},j+\frac{1}{2}} V_{\ell+\frac{1}{2},j+\frac{1}{2}}, \forall\ U, V \in \mathbb{V}_H. \tag{53}$$

Finally, we define discrete curl operators on the staggered l^2 normed spaces as

$$\begin{aligned} &\mathrm{curl_h} : \mathbb{V}_E \longrightarrow \mathbb{V}_H \\ &\mathrm{curl_h}\, \mathbf{F} := \delta_x F_y - \delta_y F_x. \end{aligned} \tag{54}$$

and

$$\begin{aligned} &\mathbf{curl_h} : \mathbb{V}_H \longrightarrow \mathbb{V}_E \\ &\mathbf{curl_h}\, U := (\delta_y U, -\delta_x U)^T. \end{aligned} \tag{55}$$

The discrete differential operators mimic properties that are satisfied by their continuous counterparts. In particular, if the PEC conditions (1e) satisfied on the discrete Yee mesh, i.e. $\forall\ \mathbf{F} \in \mathbb{V}_E$,

$$F_{x_{\ell+\frac{1}{2},0}} = F_{x_{\ell+\frac{1}{2},J}} = 0, \qquad 0 \le \ell \le L, \tag{56}$$

$$F_{y_{0,j+\frac{1}{2}}} = F_{x_{L,j+\frac{1}{2}}} = 0, \qquad 0 \le j \le J, \tag{57}$$

then discrete integrations by parts yields [14],

$$(\mathrm{curl}_h \mathbf{E}, H)_H = (\mathbf{E}, \mathbf{curl}_h H)_E. \tag{58}$$

Thus, the discrete versions of the curl operators remain adjoint to each other, which is essential for obtaining discrete energy estimates.

5.2 Yee Scheme for Maxwell-PC Debye System

To discretize the system (37), we use the same staggering in space and time as is commonly used for the free space equations. We discretize $\vec{\alpha}_x$ and $\vec{\alpha}_y$ at the same spatial grid nodes as E_x and E_y, respectively, and evaluate each at integer time steps. The time discretization of the PC Debye system (34) is performed similarly to the deterministic ODE in order to preserve second order accuracy in time. In addition, the lower order terms are discretized using a semi-implicit approximation (averaging). This allows the update steps to be essentially explicit, requiring only a tridiagonal matrix solve at each time step (which can be factored with LU factorization initially and thus only requires forward and back substitution at each time step). Using the operators defined in (44)–(47), the *Yee scheme for the Maxwell-PC Debye system* consists of the following discrete equations:

$$\delta_t H^n_{\ell+\frac{1}{2},j+\frac{1}{2}} = \frac{1}{\mu_0}\Big(\delta_y E^n_{x_{\ell+\frac{1}{2},j+\frac{1}{2}}} - \delta_x E^n_{y_{\ell+\frac{1}{2},j+\frac{1}{2}}}\Big), \tag{59a}$$

$$\epsilon_0\epsilon_\infty \delta_t E^{n+\frac{1}{2}}_{x_{\ell+\frac{1}{2},j}} = \delta_y H^{n+\frac{1}{2}}_{\ell+\frac{1}{2},j} - \delta_t \alpha^{n+\frac{1}{2}}_{0,x_{\ell+\frac{1}{2},j}}, \tag{59b}$$

$$\epsilon_0\epsilon_\infty \delta_t E^{n+\frac{1}{2}}_{y_{\ell,j+\frac{1}{2}}} = -\delta_x H^{n+\frac{1}{2}}_{\ell,j+\frac{1}{2}} - \delta_t \alpha^{n+\frac{1}{2}}_{0,y_{\ell,j+\frac{1}{2}}}, \tag{59c}$$

$$A\delta_t \vec{\alpha}^{n+\frac{1}{2}}_{x_{\ell+\frac{1}{2},j}} = \overline{\mathbf{f}}^{n+\frac{1}{2}}_{x_{\ell+\frac{1}{2},j}} - \overline{\vec{\alpha}}^{n+\frac{1}{2}}_{x_{\ell+\frac{1}{2},j}}, \tag{59d}$$

$$A\delta_t \vec{\alpha}^{n+\frac{1}{2}}_{y_{\ell,j+\frac{1}{2}}} = \overline{\mathbf{f}}^{n+\frac{1}{2}}_{y_{\ell,j+\frac{1}{2}}} - \overline{\vec{\alpha}}^{n+\frac{1}{2}}_{y_{\ell,j+\frac{1}{2}}}. \tag{59e}$$

We can re-write this system more compactly in vector form as

$$\delta_t H^n + \frac{1}{\mu_0}\left(\mathrm{curl}_h \mathbf{E}\right)^n = 0, \text{ on } \tau_h^H \tag{60a}$$

$$\epsilon_0\epsilon_\infty \delta_t \mathbf{E}^{n+\frac{1}{2}} = (\mathbf{curl}_h H)^{n+\frac{1}{2}} - \delta_t \alpha_0^{n+\frac{1}{2}}, \text{ on } \tau_h^{E_x} \times \tau_h^{E_y}, \tag{60b}$$

$$A\delta_t \vec{\alpha}^{n+\frac{1}{2}} = \overline{\mathbf{f}}^{n+\frac{1}{2}} - \overline{\vec{\alpha}}^{n+\frac{1}{2}}, \text{ on } \tau_h^{E_x} \times \tau_h^{E_y}, \tag{60c}$$

where $\alpha_0^{n+\frac{1}{2}} \in \mathbb{V}_E$, while the grid function $\vec{\alpha}$ is taken to be from the following staggered l^2 normed space

$$\mathbb{V}_\alpha := \left\{ \vec{\alpha} : \tau_h^{E_x} \times \tau_h^{E_y} \longrightarrow \mathbb{R}^2 \times \mathbb{R}^{p+1} \;\middle|\; \vec{\alpha} = [\alpha_0, \ldots, \alpha_p], \alpha_k \in \mathbb{V}_E, \|\vec{\alpha}\|_\alpha < \infty \right\},$$

where the discrete L^2 grid norm is defined as

$$\|\vec{\alpha}\|_\alpha^2 = \sum_{k=0}^{p} \|\alpha_k\|_E^2, \quad \forall\ \vec{\alpha} \in \mathbb{V}_\alpha,$$

with a corresponding inner product

$$(\vec{\alpha}, \vec{\beta})_\alpha = \sum_{k=0}^{p} \Big(\alpha_k, \beta_k\Big)_E, \quad \forall\ \vec{\alpha}, \vec{\beta} \in \mathbb{V}_\alpha.$$

5.3 Energy Decay and Stability

Here we show energy decay properties of the discrete Maxwell-PC Debye System. Energy decay implies that the method is (conditionally) stable and hence convergent. In the following we assume a uniform mesh, i.e., $\Delta x = \Delta y = h$, and that the usual CFL condition for Yee scheme is satisfied

$$\sqrt{2} c_\infty \Delta t \leq h. \tag{61}$$

Numerical demonstrations of stability in 1D for the case of uniform and Beta random relaxation times and p up to 5 was shown in [42] via a von Neumann approach.

Theorem 5.1 (Energy Decay for Maxwell-PC Debye-FDTD)**.** *If the stability condition* (61) *is satisfied, then the Yee scheme for the 2D TE mode Maxwell-PC Debye system given in* (59) *satisfies the discrete identity*

$$\delta_t \mathcal{E}_h^{n+\frac{1}{2}} = \frac{-1}{\epsilon_0 \epsilon_d \overline{\mathcal{E}}_h^{n+\frac{1}{2}}} \left\| \epsilon_0 \epsilon_d \overline{\mathbf{E}}^{n+\frac{1}{2}} \hat{\mathrm{e}}_1 - \overline{\vec{\alpha}}^{n+\frac{1}{2}} \right\|_{A^{-1}}^2, \tag{62}$$

for all n where

$$\mathcal{E}_h^n = \left(\mu_0 (H^{n+\frac{1}{2}}, H^{n-\frac{1}{2}})_H + \| \sqrt{\epsilon_0 \epsilon_\infty}\ \mathbf{E}^n \|_E^2 + \left\| \frac{1}{\sqrt{\epsilon_0 \epsilon_d}}\ \vec{\alpha}^n \right\|_\alpha^2 \right)^{1/2} \tag{63}$$

defines a discrete energy.

In the above $\|u\|_{A^{-1}}^2 := (A^{-1}u, u)_\alpha$ given A^{-1} positive definite, and $\hat{\mathrm{e}}_1$ is the first standard unit normal vector of length $p+1$.

Note that $\|\vec{\alpha}\|_\alpha^2 \approx \|\mathbb{E}[\mathcal{P}]\|_2^2 + \|\mathrm{StdDev}(\mathcal{P})\|_2^2 = \mathbb{E}[\|\mathcal{P}\|_2^2] = \|\mathcal{P}\|_F^2$ so that this is a natural extension of the Maxwell-Random Debye energy (24).

Proof. We follow the proof in [14] which proves stability of the Yee scheme for the Maxwell-Debye system using energy techniques.

We first note that the equations for the polarization in the PC Debye system (59d) and (59e) can be re-written as

$$\delta_t \vec{\alpha}_{x_{\ell+\frac{1}{2},j}}^{n+\frac{1}{2}} = \epsilon_0 \epsilon_d \overline{E}_{x_{\ell+\frac{1}{2},j}}^{n+\frac{1}{2}} A^{-1} \hat{\mathrm{e}}_1 - A^{-1} \overline{\vec{\alpha}}_{x_{\ell+\frac{1}{2},j}}^{n+\frac{1}{2}}, \tag{64a}$$

$$\delta_t \vec{\alpha}_{y_{\ell,j+\frac{1}{2}}}^{n+\frac{1}{2}} = \epsilon_0 \epsilon_d \overline{E}_{y_{\ell,j+\frac{1}{2}}}^{n+\frac{1}{2}} A^{-1} \hat{\mathrm{e}}_1 - A^{-1} \overline{\vec{\alpha}}_{y_{\ell,j+\frac{1}{2}}}^{n+\frac{1}{2}} \tag{64b}$$

or in vector form as

$$\delta_t \vec{\alpha}^{n+\frac{1}{2}} = \epsilon_0 \epsilon_d \overline{\mathbf{E}}^{n+\frac{1}{2}} A^{-1} \hat{\mathrm{e}}_1 - A^{-1} \overline{\vec{\alpha}}^{n+\frac{1}{2}}. \tag{65}$$

We substitute these into the equations for the electric field (59b) and (59c) and re-write as

$$\epsilon_0\epsilon_\infty\delta_t E^{n+\frac{1}{2}}_{x_{\ell+\frac{1}{2},j}} = \delta_y H^{n+\frac{1}{2}}_{\ell+\frac{1}{2},j} - \epsilon_0\epsilon_d(\hat{\mathrm{e}}_1^T A^{-1}\hat{\mathrm{e}}_1)\overline{E}^{n+\frac{1}{2}}_{x_{\ell+\frac{1}{2},j}} + \left(\hat{\mathrm{e}}_1^T A^{-1}\overline{\vec{\alpha}}^{n+\frac{1}{2}}_{x_{\ell+\frac{1}{2},j}}\right), \tag{66a}$$

$$\epsilon_0\epsilon_\infty\delta_t E^{n+\frac{1}{2}}_{y_{\ell,j+\frac{1}{2}}} = -\delta_x H^{n+\frac{1}{2}}_{\ell,j+\frac{1}{2}} - \epsilon_0\epsilon_d(\hat{\mathrm{e}}_1^T A^{-1}\hat{\mathrm{e}}_1)\overline{E}^{n+\frac{1}{2}}_{y_{\ell,j+\frac{1}{2}}} + \left(\hat{\mathrm{e}}_1^T A^{-1}\overline{\vec{\alpha}}^{n+\frac{1}{2}}_{y_{\ell,j+\frac{1}{2}}}\right), \tag{66b}$$

or in vector form as

$$\epsilon_0\epsilon_\infty\delta_t\mathbf{E}^{n+\frac{1}{2}} = \mathbf{curl}_{\mathrm{h}}\, H^{n+\frac{1}{2}} - \epsilon_0\epsilon_d(\hat{\mathrm{e}}_1^T A^{-1}\hat{\mathrm{e}}_1)\overline{\mathbf{E}}^{n+\frac{1}{2}} + \hat{\mathrm{e}}_1^T A^{-1}\overline{\vec{\alpha}}^{n+\frac{1}{2}}. \tag{67}$$

Multiplying both sides of (67) by $\Delta x\Delta y\overline{\mathbf{E}}^{n+\frac{1}{2}}$ and summing over all spatial nodes on $\tau_h^{E_x}\times\tau_h^{E_y}$ we obtain

$$\begin{aligned}\epsilon_0\epsilon_\infty(\delta_t\mathbf{E}^{n+\frac{1}{2}},\overline{\mathbf{E}}^{n+\frac{1}{2}})_E = (\mathbf{curl}_{\mathrm{h}}\, H^{n+\frac{1}{2}},\overline{\mathbf{E}}^{n+\frac{1}{2}})_E \\ - \epsilon_0\epsilon_d(\hat{\mathrm{e}}_1^T A^{-1}\hat{\mathrm{e}}_1)(\overline{\mathbf{E}}^{n+\frac{1}{2}},\overline{\mathbf{E}}^{n+\frac{1}{2}})_E + \left(\hat{\mathrm{e}}_1^T A^{-1}\overline{\vec{\alpha}}^{n+\frac{1}{2}},\overline{\mathbf{E}}^{n+\frac{1}{2}}\right)_E\end{aligned} \tag{68}$$

which can be re-written as

$$\begin{aligned}\frac{\epsilon_0\epsilon_\infty}{2\Delta t}\left[\|\mathbf{E}^{n+1}\|_E^2 - \|\mathbf{E}^n\|_E^2\right] = (\mathbf{curl}_h H^{n+\frac{1}{2}},\overline{\mathbf{E}}^{n+\frac{1}{2}})_E \\ - \epsilon_0\epsilon_d(\hat{\mathrm{e}}_1^T A^{-1}\hat{\mathrm{e}}_1)\|\overline{\mathbf{E}}^{n+\frac{1}{2}}\|_E^2 + \left(\hat{\mathrm{e}}_1^T A^{-1}\overline{\vec{\alpha}}^{n+\frac{1}{2}},\overline{\mathbf{E}}^{n+\frac{1}{2}}\right)_E.\end{aligned} \tag{69}$$

We consider the average of (60a) at n and $n+1$, multiply with $\Delta x\Delta y H^{n+\frac{1}{2}}$ and sum over all spatial nodes on τ_h^H to get

$$\mu_0(\overline{\delta_t H}^{n+\frac{1}{2}},H^{n+\frac{1}{2}})_H + (\overline{\mathrm{curl}_h\mathbf{E}}^{n+\frac{1}{2}},H^{n+\frac{1}{2}})_H = 0. \tag{70}$$

We can rewrite (70) as

$$\frac{\mu_0}{2\Delta t}\left[(H^{n+\frac{3}{2}},H^{n+\frac{1}{2}})_H - (H^{n+\frac{1}{2}},H^{n-\frac{1}{2}})_H\right] + (\overline{\mathrm{curl}_{\mathrm{h}}\mathbf{E}}^{n+\frac{1}{2}},H^{n+\frac{1}{2}})_H = 0. \tag{71}$$

Finally, we multiply equation (65) by $\Delta x\Delta y\ \overline{\vec{\alpha}}^{n+\frac{1}{2}}$ and sum over all spatial nodes on $\tau_h^{E_x}\times\tau_h^{E_y}$ as well as all degrees $k=0,\ldots,p$ to get

$$\left(\delta_t\vec{\alpha}^{n+\frac{1}{2}},\overline{\vec{\alpha}}^{n+\frac{1}{2}}\right)_\alpha = \epsilon_0\epsilon_d\left(\overline{\mathbf{E}}^{n+\frac{1}{2}}A^{-1}\hat{\mathrm{e}}_1,\overline{\vec{\alpha}}^{n+\frac{1}{2}}\right)_\alpha - \left(A^{-1}\overline{\vec{\alpha}}^{n+\frac{1}{2}},\overline{\vec{\alpha}}^{n+\frac{1}{2}}\right)_\alpha, \tag{72}$$

which can be re-written as

$$\frac{1}{2\Delta t\epsilon_0\epsilon_d}\left[\|\vec{\alpha}^{n+1}||_\alpha^2 - \|\vec{\alpha}^n\|_\alpha^2\right] = \left(\overline{\mathbf{E}}^{n+\frac{1}{2}}A^{-1}\hat{\mathrm{e}}_1,\overline{\vec{\alpha}}^{n+\frac{1}{2}}\right)_\alpha - \frac{1}{\epsilon_0\epsilon_d}\left(A^{-1}\overline{\vec{\alpha}}^{n+\frac{1}{2}},\overline{\vec{\alpha}}^{n+\frac{1}{2}}\right)_\alpha. \tag{73}$$

Adding equations (69), (71), and (73), and using the definition (63) we have

$$\frac{1}{2\Delta t}\left\{(\mathcal{E}_h^{n+1})^2-(\mathcal{E}_h^n)^2\right\}=\left(\overline{\mathbf{E}}^{n+\frac{1}{2}}A^{-1}\hat{\mathrm{e}}_1,\overline{\vec{\alpha}}^{n+\frac{1}{2}}\right)_\alpha-\frac{1}{\epsilon_0\epsilon_d}\left(A^{-1}\overline{\vec{\alpha}}^{n+\frac{1}{2}},\overline{\vec{\alpha}}^{n+\frac{1}{2}}\right)_\alpha$$
$$-\epsilon_0\epsilon_d(\hat{\mathrm{e}}_1^TA^{-1}\hat{\mathrm{e}}_1)\left\|\overline{\mathbf{E}}^{n+\frac{1}{2}}\right\|_E^2+\left(\hat{\mathrm{e}}_1^TA^{-1}\overline{\vec{\alpha}}^{n+\frac{1}{2}},\overline{\mathbf{E}}^{n+\frac{1}{2}}\right)_E \tag{74}$$
$$=-\frac{1}{\epsilon_0\epsilon_d}\Big[\left(A^{-1}\overline{\vec{\alpha}}^{n+\frac{1}{2}},\overline{\vec{\alpha}}^{n+\frac{1}{2}}\right)_\alpha-2\epsilon_0\epsilon_d\left(\overline{\mathbf{E}}^{n+\frac{1}{2}}A^{-1}\hat{\mathrm{e}}_1,\overline{\vec{\alpha}}^{n+\frac{1}{2}}\right)_\alpha$$
$$+(\epsilon_0\epsilon_d)^2(\hat{\mathrm{e}}_1^TA^{-1}\hat{\mathrm{e}}_1)\left\|\overline{\mathbf{E}}^{n+\frac{1}{2}}\right\|_E^2\Big] \tag{75}$$
$$=-\frac{1}{\epsilon_0\epsilon_d}\Big(A^{-1}(\overline{\vec{\alpha}}^{n+\frac{1}{2}}-\epsilon_0\epsilon_d\overline{\mathbf{E}}^{n+\frac{1}{2}}\hat{\mathrm{e}}_1),\overline{\vec{\alpha}}^{n+\frac{1}{2}}-\epsilon_0\epsilon_d\overline{\mathbf{E}}^{n+\frac{1}{2}}\hat{\mathrm{e}}_1\Big)_\alpha. \tag{76}$$

We can rewrite this equation in the form

$$\frac{\mathcal{E}_h^{n+1}-\mathcal{E}_h^n}{\Delta t}=-\left(\frac{2}{\mathcal{E}_h^{n+1}+\mathcal{E}_h^n}\right)\frac{1}{\epsilon_0\epsilon_d}\left\|\epsilon_0\epsilon_d\overline{\mathbf{E}}^{n+\frac{1}{2}}\hat{\mathrm{e}}_1-\overline{\vec{\alpha}}^{n+\frac{1}{2}}\right\|_{A^{-1}}^2, \tag{77}$$

where $\|u\|_{A^{-1}}^2:=(A^{-1}u,u)_\alpha$ given A^{-1} positive definite. Upon utilizing the definitions of the time differencing and averaging operators in (44) and (45), respectively, we have the discrete identity (62) for the Maxwell-PC Debye system.

What is left to prove is that the quantity defined in (63) is a discrete energy, i.e., a positive definite function of the solution to the system (59). This involves recognizing that the energy can alternatively be written as

$$(\mathcal{E}_h^n)^2=\mu_0\|\overline{H}^n\|_H^2+\epsilon_0\epsilon_\infty(E^n,\mathcal{A}_hE^n)_E+\frac{1}{\epsilon_0\epsilon_d}\Big(A^{-1}(\vec{\alpha}^n-\epsilon_0\epsilon_d\mathbf{E}^n\hat{\mathrm{e}}_1),\vec{\alpha}^n-\epsilon_0\epsilon_d\mathbf{E}^n\hat{\mathrm{e}}_1\Big)_\alpha$$

which is positive definite since $\mathcal{A}_h$ positive definite when the CFL condition is satisfied [14], and A^{-1} is always positive definite (Remark 4.1). □

5.4 Discrete Dispersion Relation

In [47] it was shown that for the Yee scheme applied to the (deterministic) Maxwell-Debye, the *discrete dispersion relation* can be written

$$\frac{\omega_\Delta^2}{c^2}\epsilon_\Delta(\omega)=K_\Delta^2 \tag{78}$$

where the *discrete complex permittivity* is given by

$$\epsilon_\Delta(\omega)=\epsilon_\infty+\epsilon_d\left(\frac{1}{1-\mathrm{i}\omega_\Delta\tau_\Delta}\right)$$

with discrete representations of ω and τ given by

$$\omega_\Delta=\frac{\sin(\omega\Delta t/2)}{\Delta t/2},\qquad \tau_\Delta=\sec(\omega\Delta t/2)\tau.$$

The quantity K_Δ relates the spatial discretization scheme to the resulting numerical wave vector $\vec{k}_\Delta=[k_{x,\Delta},k_{y,\Delta},k_{z,\Delta}]^T$. For example, in 2D

$$K_\Delta:=\left(\sum_{w\in\{x,y\}}K_{w,\Delta}^2\right)^{1/2}$$

where $K_{w,\Delta}, w \in \{x, y\}$ is related to the *symbol of the discrete first order spatial difference operator* by [13]

$$\mathrm{i}K_{w,\Delta} = \mathcal{F}(\mathcal{D}_{1,\Delta w}).$$

i.e.,

$$K_{w,\Delta} := \frac{\sin\left(k_{w,\Delta}\ \Delta w/2\right)}{\Delta w/2}, \quad w \in \{x, y\}.$$

It is clear from (78) that the left hand side of the discrete dispersion relation depends on the polarization model, dielectric parameters and the choice of time discretization, while the right hand side depends on the number of spatial dimensions and the choice of spatial discretization, e.g., higher order finite difference approximations [13, 15].

Theorem 5.2. *The* discrete dispersion relation *for the Maxwell-PC Debye FDTD scheme in* (59) *can be written as* (78) *where the* discrete expected complex permittivity *is given by*

$$\epsilon_\Delta(\omega) := \epsilon_\infty + \epsilon_d \hat{e}_1^T \left(I - \mathrm{i}\omega_\Delta A_\Delta\right)^{-1} \hat{e}_1,$$

and the discrete PC matrix *is given by*

$$A_\Delta := \sec(\omega\Delta t/2) A.$$

In the above, definitions of the quantities ω_Δ and K_Δ are the same as before. Note that the same relation holds in 1 and 3D, as well as with higher order accurate spatial difference operators.

Recall that the exact *expected complex permittivity* is given by

$$\epsilon(\omega) = \epsilon_\infty + \epsilon_d \mathbb{E}\left[\frac{1}{1 - \mathrm{i}\omega\tau}\right].$$

Proof. We assume plane wave solutions of the form

$$V_{\ell,j}^n = \tilde{V} \mathrm{e}^{\mathrm{i}\left(\ell\Delta x k_{x,\Delta} + j\Delta y k_{y,\Delta} - \omega n \Delta t\right)}$$

for each of $V = H, E_x, E_y, \alpha_{x,0}, \ldots, \alpha_{x,p}, \alpha_{y,0}, \ldots, \alpha_{y,p}$. We substitute these representations into (59), cancel like terms and simplify to obtain

$$\tilde{H}\sin(\omega\Delta t/2) + \frac{\Delta t}{\mu_0 \Delta y}\tilde{E}_x \sin(k_{y,\Delta}\Delta y/2) - \frac{\Delta t}{\mu_0 \Delta x}\tilde{E}_y \sin(k_{x,\Delta}\Delta x/2) = 0, \tag{79a}$$

$$\left(\epsilon_0\epsilon_\infty \tilde{E}_x + \tilde{\alpha}_{x,0}\right)\sin(\omega\Delta t/2) + \frac{\Delta t}{\Delta y}\tilde{H}\sin(k_{y,\Delta}\Delta y/2) = 0, \tag{79b}$$

$$\left(\epsilon_0\epsilon_\infty \tilde{E}_y + \tilde{\alpha}_{y,0}\right)\sin(\omega\Delta t/2) + \frac{\Delta t}{\Delta x}\tilde{H}\sin(k_{x,\Delta}\Delta x/2) = 0, \tag{79c}$$

$$A\tilde{\vec{\alpha}}_x \left(\frac{-2\mathrm{i}}{\Delta t}\sin(\omega\Delta t/2)\right) + \cos(\omega\Delta t/2)\tilde{\vec{\alpha}}_x - \epsilon_0\epsilon_d \tilde{E}_x \cos(\omega\Delta t/2)\hat{e}_1 = 0, \tag{79d}$$

$$A\tilde{\vec{\alpha}}_y \left(\frac{-2\mathrm{i}}{\Delta t}\sin(\omega\Delta t/2)\right) + \cos(\omega\Delta t/2)\tilde{\vec{\alpha}}_y - \epsilon_0\epsilon_d \tilde{E}_y \cos(\omega\Delta t/2)\hat{e}_1 = 0, \tag{79e}$$

where $\tilde{\vec{\alpha}}_w := [\tilde{\alpha}_{w,0}, \ldots, \tilde{\alpha}_{w,p}]^T$, $w \in \{x, y\}$. Equations (79d) and (79e) can be re-written in terms of discrete parameters as

$$\left(I - \mathrm{i}\omega_\Delta A_\Delta\right)\tilde{\vec{\alpha}}_w = \epsilon_0\epsilon_d \tilde{E}_w \hat{e}_1, \quad w \in \{x, y\},$$

which allows one to solve explicitly for

$$\tilde{\alpha}_{w,0} = \epsilon_0 \epsilon_d \tilde{E}_w \hat{e}_1^T \left(I - \mathrm{i}\omega_\Delta A_\Delta\right)^{-1} \hat{e}_1, \quad w \in \{x, y\}. \tag{80}$$

which we in to equations (79b) and (79c) to get

$$\epsilon_0 \epsilon_\Delta(\omega) \tilde{E}_x \omega_\Delta = -K_{y,\Delta} \tilde{H}, \tag{81}$$

$$\epsilon_0 \epsilon_\Delta(\omega) \tilde{E}_y \omega_\Delta = K_{x,\Delta} \tilde{H}. \tag{82}$$

Finally, we solve (81) for $\tilde{E}_x$, solve (82) for $\tilde{E}_y$, and substitute these into (79a) to obtain the desired relation. □

5.5 Dispersion Error

We define the phase error Φ for any method applied to a particular model to be

$$\Phi = \left| \frac{k_{\mathrm{EX}} - k_\Delta}{k_{\mathrm{EX}}} \right|, \tag{83}$$

where the numerical wave number $k_\Delta := \|\vec{k}_\Delta\|$ is implicitly determined by the corresponding dispersion relation and k_{EX} is the exact wave number for the given model. We wish to examine the phase error as a function of $\omega\Delta t$ in the range $[0, \pi]$, however the range $[0, \pi/4]$ is more practical since $\omega\Delta t = 2\pi/N_{\mathrm{ppp}}$, where N_{ppp} is the number of points per period. In the plots below, we have assumed the following parameters which are appropriate constants for modeling aqueous materials:

$$\epsilon_\infty = 1, \quad \epsilon_s = 78.2, \quad \tau_m = 8.1 \times 10^{-12} \text{ sec.}$$

We investigate *narrow* and *wide* distributions by allowing $\tau_r = 0.5\tau_m$ and $\tau_r = 0.9\tau_m$. We allow *low*, *medium* and *high* resolution by choosing $h_\tau := \tau_m/\Delta t$ to be 0.1, 0.01, and 0.0001, while the spatial mesh is determined by satisfying the CFL condition (61). Figure 5.5 shows several plots of phase error at zero angle of incidence ($\theta = 0$), for various polynomial chaos degrees M. Note that degree 0 is the deterministic case, therefore these curves represent the error in not accounting for distributions of relaxation times when they are present in the material. It is striking that reducing the discretization parameters (e.g., Δt) can actually increase the phase error in the highest resolution case, unless the random Debye model is fully resolved.

In Figure 5.5 we show several log plots of phase error versus angle of incidence (θ) with fixed $\omega = 1/\tau_m$. For the wide distributions, a higher degree (M) of the polynomial chaos expansion is needed to achieve convergence. As in Figure 5.5 we see that the high PC degree approximations attain lower error only for the high resolution examples. Further, only the highest degree approximation in each plot exhibits a dependence on θ, indicating that the errors in the temporal, spatial and PC approximations are additive.

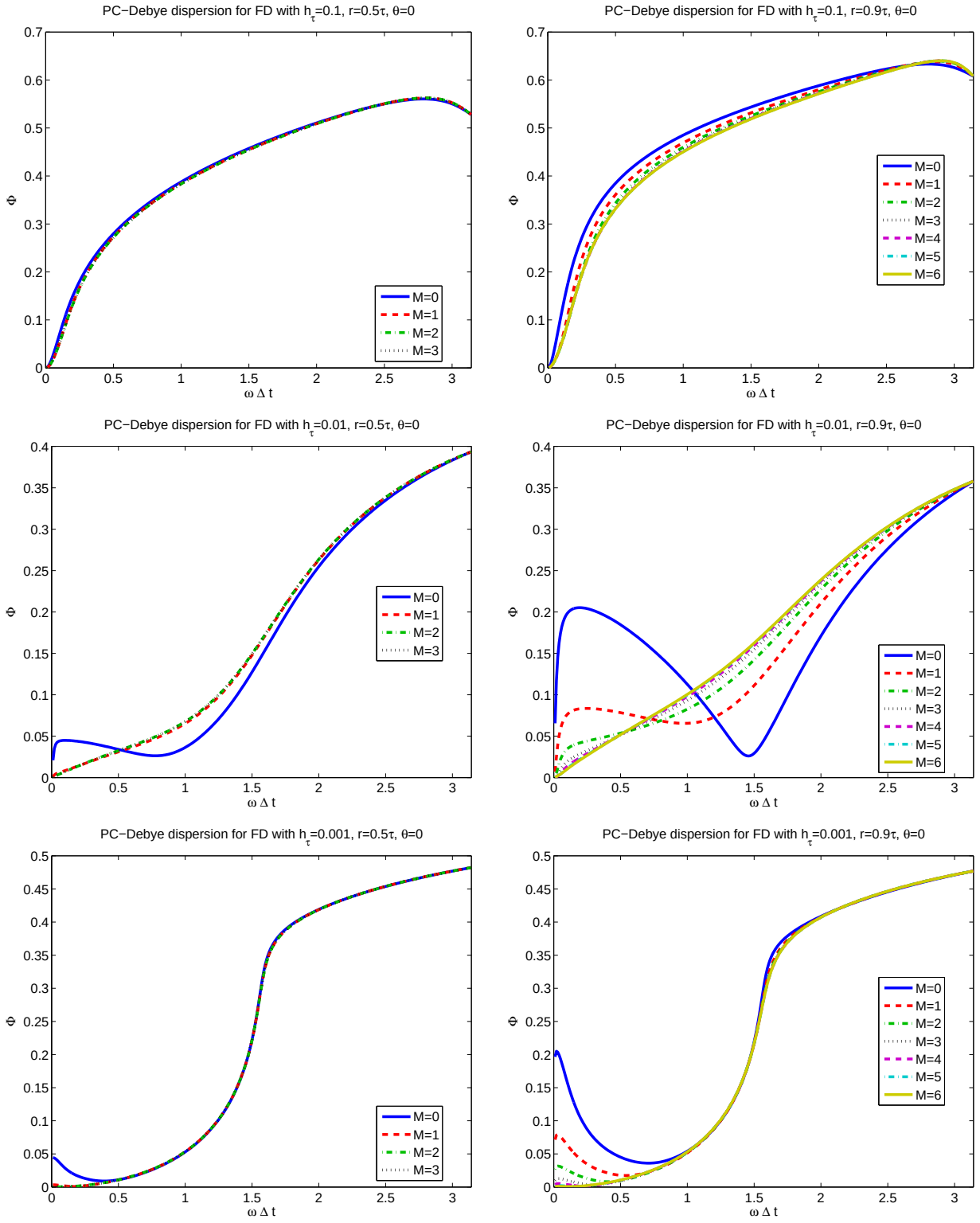

Figure 1: Plots of phase error at $\theta = 0$ for (left column) $\tau_r = 0.5\tau_m$, (right column) $\tau_r = 0.9\tau_m$, (top row) $h_\tau = 0.1$, (middle row) $h_\tau = 0.01$, (bottom row) $h_\tau = 0.001$.

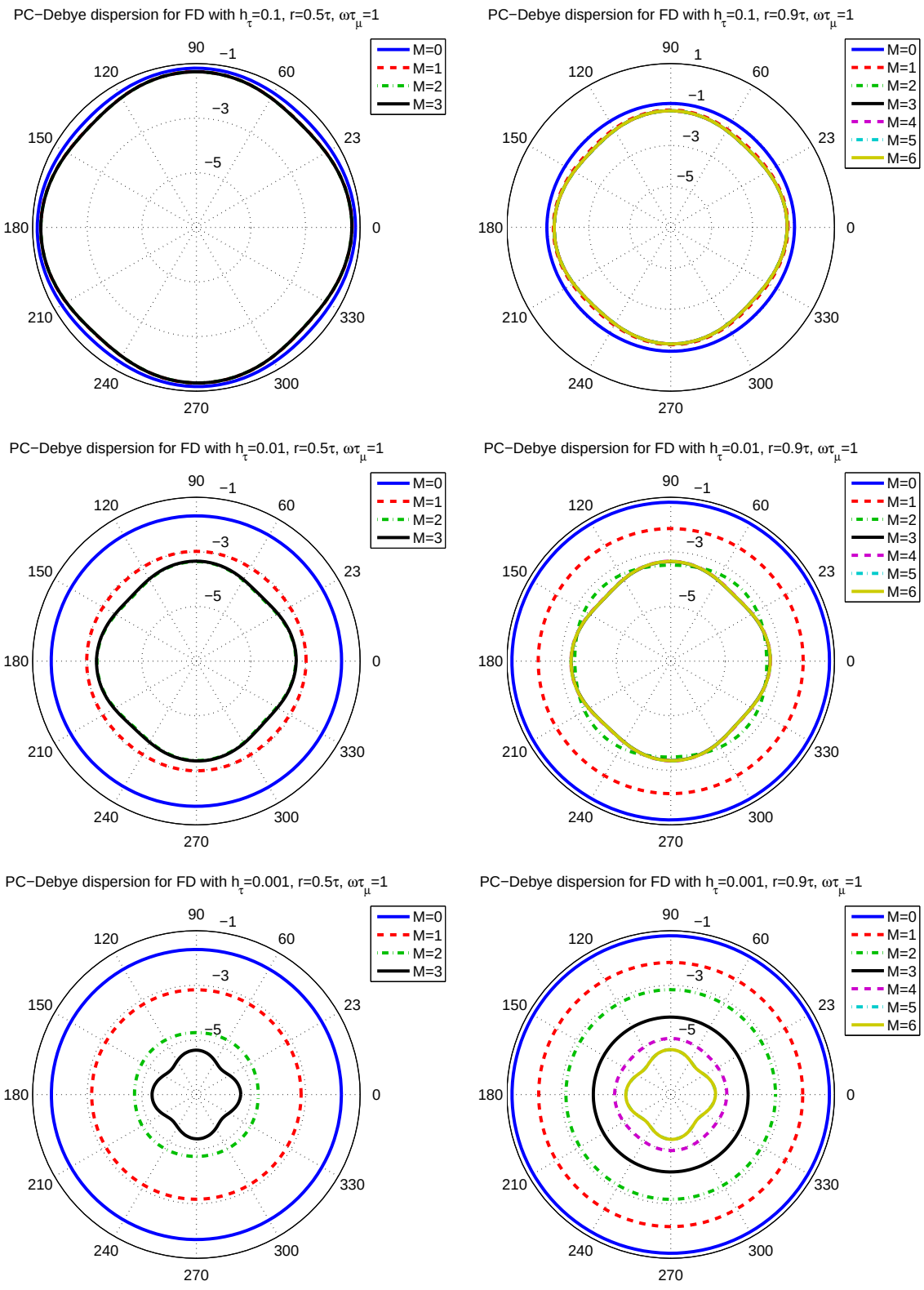

Figure 2: Log plots of phase error versus θ with fixed $\omega = 1/\tau_m$ for (left column) $\tau_r = 0.5\tau_m$, (right column) $\tau_r = 0.9\tau_m$, (top row) $h_\tau = 0.1$, (middle row) $h_\tau = 0.01$, (bottom row) $h_\tau = 0.001$. Legend indicates degree M of the PC expansion.

6 Conclusions

In this work we have discussed theoretical and numerical results for Maxwell's equations with a Debye polarization term which includes probability distributions for the relaxation time. We applied the Polynomial Chaos technique to discretize in random space the auxiliary ordinary differential equation for polarization. A similar approach can apply to other polarization models such as Lorentz, or Drude. Combinations of polarization mechanisms can also be handled in a straightforward manner, including multi-pole Debye or mixtures of materials.

In [42], it was shown that one can improve the traditional Debye model by replacing the average relaxation time $\bar{\tau}$ with a distribution of relaxation times. The method of Polynomial Chaos Expansions provides us with a convenient means of representing the random polarization, $\mathcal{P}$ as a linear combination of orthogonal polynomials. By projecting into finite random space, we are able to replace a random ordinary differential equation with a system of deterministic ODEs. Combining these with Maxwell's equations and noting that the electric field E depends only on the macroscopic polarization $\mathbb{E}(P) \approx \alpha_0$, we obtain the polynomial chaos model (34) for an electromagnetic field propagating through a dispersive dielectric media.

This model lends itself naturally to discretization using the Yee scheme with an additional central difference approximation for the Polynomial Chaos system. From the discretized equations, one is able to obtain a series of sequential (nearly) explicit update equations, requiring only a tridiagonal (static) matrix solve for the polarization at each time step.

We have shown that the approach maintains the conditional stability of the Yee scheme for Debye materials. We have also derived the discrete dispersion relation which allows the phase error to be computed. This is helpful in that it can provide a quick heuristic for how to relate the degree of the Polynomial Chaos Expansion to the temporal and spatial discretization parameters in order to balance error contributions.

7 Acknowledgments

Aspects of this work were completed by the author while advising undergraduate students in the Mathematics REU Program at Oregon State University, funded by NSF-DMS Grant No. 0852030.

References

[1] R. A. Albanese, J. W. Penn, and R. L. Medina. Short-rise-time microwave pulse propagation through dispersive biological media. *J. Opt. Soc. Amer. A*, 6:1441–1446, 1989.

[2] M. Armentrout and N. L. Gibson. Electromagnetic relaxation time distribution inverse problems in the time-domain. In *WAVES International Conference Proceedings*, 2011.

[3] H Banks and V Bokil. A computational and statistical framework for multidimensional domain acoustooptic material interrogation. *Quarterly of Applied Mathematics*, 63(1):156–200, 2005.

[4] H. T. Banks, M. W. Buksas, and T. Lin. *Electromagnetic Material Interrogation Using Conductive Interfaces and Acoustic Wavefronts*, volume FR21 of *Frontiers in Applied Mathematics*. SIAM, Philadelphia, PA, 2000.

[5] H. T. Banks and N. L. Gibson. Well-posedness in Maxwell systems with distributions of polarization relaxation parameters. *Appl. Math. Let.*, 18(4):423–430, 2005.

[6] H. T. Banks and N. L. Gibson. Electromagnetic inverse problems involving distributions of dielectric mechanisms and parameters. *Quarterly of Appl. Math.*, 64(4):749–795, 2006.

[7] HT Banks, Nathan L Gibson, and William P Winfree. Gap detection with electromagnetic terahertz signals. *Nonlinear Analysis: Real World Applications*, 6(2):381–416, 2005.

[8] I. Barba, A. C. L. Cabeceira, M. Panizo, and J. Represa. Modelling dispersive dielectrics in TLM method. *Int. J. Numer. Model.*, 14:15–30, 2001.

[9] K. Barrese and N. Chugh. Approximating dispersive mechanisms using the debye model with distributed dielectric parameters. In N. L. Gibson, editor, *REU Program at Oregon State University Proceedings*, 2008.

[10] RS Beezley and RJ Krueger. An electromagnetic inverse problem for dispersive media. *Journal of mathematical physics*, 26:317, 1985.

[11] E. Bela and E. Hortsch. Generalized polynomial chaos and dispersive dielectric media. In N. L. Gibson, editor, *REU Program at Oregon State University Proceedings*, 2010.

[12] A Bello, E Laredo, and M Grimau. Distribution of relaxation times from dielectric spectroscopy using monte carlo simulated annealing: application to α-pvdf. *Physical Review B*, 60(18):12764, 1999.

[13] V. A. Bokil and N. L. Gibson. Analysis of spatial high-order finite difference methods for maxwell's equations in dispersive media. *IMA Journal of Numerical Analysis*, 32(3):926–956, 2012.

[14] V. A. Bokil and N. L. Gibson. Convergence analysis of Yee schemes for Maxwell's equations in Debye and Lorentz dispersive media. Technical report, Oregon State University, http://hdl.handle.net/1957/38475, 2013. Submitted.

[15] V. A. Bokil and N. L. Gibson. Stability and dispersion analysis of high order FDTD methods for maxwell's equations in dispersive media. In *Recent Advances in Scientific Computing and Applications*, volume 586 of *Contemporary Mathematics*, pages 73–82. American Mathematical Soc., 2013.

[16] C. J. F. Böttcher and P. Bordewijk. *Theory of electric polarization*, volume II. Elsevier Amsterdam, 1978.

[17] M.F. Causley, P.G. Petropoulos, and S. Jiang. Incorporating the Havriliak-Negami dielectric model in the FD-TD method. *Journal of Computational Physics*, 2011.

[18] Cédric Chauvière, Jan S Hesthaven, and L Lurati. Computational modeling of uncertainty in time-domain electromagnetics. *SIAM Journal on Scientific Computing*, 28(2):751–775, 2006.

[19] K. S. Cole and R. H. Cole. Dispersion and absorption in dielectrics I. alternating current characteristics. *J. Chem. Phy.*, 9:341–351, 1941.

[20] P. J. W. Debye. *Polar molecules*. The Chemical Catalog Company, Inc., 1929.

[21] S. Ellingsrud, T. Eidesmo, S. Johansen, MC Sinha, LM MacGregor, and S. Constable. Remote sensing of hydrocarbon layers by seabed logging (SBL): Results from a cruise offshore Angola. *The Leading Edge*, 21(10):972, 2002.

[22] E. C. Fear, P. M. Meaney, and M. A. Stuchly. Microwaves for breast cancer detection. *IEEE Potentials*, pages 12–18, 2003.

[23] K. R. Foster and H. P. Schwan. Dielectric properties of tissues and biological materials: A critical review. *Critical Rev. in Biomed. Engr.*, 17:25–104, 1989.

[24] K. R. Foster and H. P. Schwan. Dielectric properties of tissues. *Handbook of biological effects of electromagnetic fields*, 2:25–102, 1996.

[25] P. Fuks, A. Karlsson, and G. Larson. Direct and inverse scattering from dispersive media. *Inverse Problems*, 10:555, 1994.

[26] C. Gabriel. Compilation of the dielectric properties of body tissues at RF and microwave frequencies. Technical Report AL/OE-TR-1996-0037, USAF Armstrong Laboratory, Brooks AFB, TX, 1996.

[27] C. Gabriel, S. Gabriel, and E. Corthout. The dielectric properties of biological tissues: I. literature survey. *Physics in medicine and biology*, 41:2231–2249, 1996.

[28] S. Gabriel, R. W. Lau, and C. Gabriel. The dielectric properties of biological tissues: II. measurements in the frequency range 10 Hz to 20 GHz. *Physics in medicine and biology*, 41:2251–2269, 1996.

[29] S. Gabriel, R. W. Lau, and C. Gabriel. The dielectric properties of biological tissues: III. parametric models for the dielectric spectrum of tissues. *Physics in medicine and biology*, 41:2271–2293, 1996.

[30] Gene H Golub and John H Welsch. Calculation of gauss quadrature rules. *Mathematics of Computation*, 23(106):221–230, 1969.

[31] W. D. Hurt. Multiterm debye dispersion relations for permittivity of muscle. *Biomedical Engineering, IEEE Transactions on*, (1):60–64, 1985.

[32] R. M. Joseph, S. C. Hagness, and A. Taflove. Direct time integration of Maxwell's equations in linear dispersive media with absorption for scattering and propagation of femtosecond electromagnetic pulses. *Optics Lett.*, 16(18):1412–1414, 1991.

[33] R. M. Joseph and A. Taflove. FDTD maxwell's equations models for nonlinear electrodynamics and optics. *Antennas and Propagation, IEEE Transactions on*, 45(3):364–374, 1997.

[34] T. Kashiwa and I. Fukai. A treatment by the FD-TD method of the dispersive characteristics associated with electronic polarization. *Microwave Opt. Technol. Lett.*, 3(6):203–205, 1990.

[35] T. Kashiwa, N. Yoshida, and I. Fukai. A treatment by the finite-difference time domain method of the dispersive characteristics associated with orientational polarization. *IEEE Transactions of the IEICE*, 73(8):1326–1328, 1990.

[36] David F Kelley and Raymond J Luebbers. Debye function expansions of empirical models of complex permittivity for use in FDTD solutions. In *Antennas and Propagation Society International Symposium, 2003. IEEE*, volume 4, pages 372–375. IEEE, 2003.

[37] S. Lanteri and C. Scheid. Convergence of a discontinuous Galerkin scheme for the mixed time-domain Maxwell's equations in dispersive media. *IMA Journal of Numerical Analysis*, 2012.

[38] J. Li. Unified analysis of leap-frog methods for solving time-domain Maxwell's equations in dispersive media. *Journal of Scientific Computing*, 47(1):1–26, 2011.

[39] Jichun Li, Yunqing Huang, and Yanping Lin. Developing finite element methods for Maxwell's equations in a Cole-Cole dispersive medium. *SIAM Journal on Scientific Computing*, 33(6):3153–3174, 2011.

[40] R. Luebbers, F. P. Hunsberger, K. S. Kunz, R. B. Standler, and M. Schneider. A frequency-dependent finite-difference time-domain formulation for dispersive materials. *IEEE Trans. Electromagnetic Compatibility*, 32(3):222–227, 1990.

[41] GI Metternicht and JA Zinck. Remote sensing of soil salinity: potentials and constraints. *Remote Sensing of Environment*, 85(1):1–20, 2003.

[42] M. Milne and D. Wedde. Simulating polydisperse materials with distributions of the debye model. In N. L. Gibson, editor, *REU Program at Oregon State University Proceedings*, 2009.

[43] N. Miura, S. Yagihara, and S. Mashimo. Microwave dielectric properties of solid and liquid foods investigated by time-domain reflectometry. *Journal of food science*, 68(4):1396–1403, 2003.

[44] P. Monk. A comparison of three mixed methods for the time-dependent Maxwell's equations. *SIAM Sci. Stat. Comput.*, 13:1097–1122, 1992.

[45] P. Monk. *Finite Element Methods for Maxwell's Equations*. Oxford University Press, 2003.

[46] Peter Monk. A convergence analysis of Yee's scheme on nonuniform grids. *SIAM J. Numer. Anal.*, 31(2):393–412, April 1994.

[47] P. G. Petropoulos. Stability and phase error analysis of FD-TD in dispersive dielectrics. *IEEE Trans. Antennas Propagat.*, 42(1):62–69, 1994.

[48] P.G. Petropoulos. On the time-domain response of Cole-Cole dielectrics. *Antennas and Propagation, IEEE Transactions on*, 53(11):3741–3746, 2005.

[49] JD Shea, P. Kosmas, BD Van Veen, and SC Hagness. Contrast-enhanced microwave imaging of breast tumors: a computational study using 3D realistic numerical phantoms. *Inverse problems*, 26:074009, 2010.

[50] J.D. Shea, B.D. VanVeen, and S.C. Hagness. A TSVD analysis of microwave inverse scattering for breast imaging. *Biomedical Engineering, IEEE Transactions on*, (99):1–1, 2011.

[51] R. Siushansian and LoVetri J. A comparison of numerical techniques for modeling electromagnetic dispersive media. *IEEE Microwave Guided Wave Lett.*, 5:426–428, 1995.

[52] Pavel Ŝolín. *Partial differential equations and the finite element method*, volume 73. Wiley, 2005.

[53] J. C. Strikverda. *Finite Difference Schemes and Partial Differential Equations*. SIAM, 2004.

[54] A. Taflove and S. C. Hagness. *Computational Electrodynamics: The Finite-Difference Time-Domain method*. Artech House, Norwood, MA, 3rd edition, 2005.

[55] Andrey Tarasov and Konstantin Titov. Relaxation time distribution from time domain induced polarization measurements. *Geophysical Journal International*, 170(1):31–43, 2007.

[56] M-R Tofighi. FDTD modeling of biological tissues cole–cole dispersion for 0.5–30 ghz using relaxation time distribution samplesnovel and improved implementations. *Microwave Theory and Techniques, IEEE Transactions on*, 57(10):2588–2596, 2009.

[57] E. R. v. Schweidler. Studien über anomalien im verhalten der dielektrika. *Annalen der Physik*, 329(14):711–770, 1907.

[58] K.W. Wagner. Zur theorie der unvollkommenen dielektrika. *Annalen der Physik*, 345(5):817–855, 1913.

[59] LV Wolfersdorf. On an electromagnetic inverse problem for dispersive media. *Quarterly of Applied Mathematics*, 49:237–246, 1991.

[60] D. Xiu and G.E. Karniadakis. The Wiener–Askey polynomial chaos for stochastic differential equations. *SIAM Journal on Scientific Computing*, 24(2):619–644, 2003.

[61] Dongbin Xiu. *Numerical Methods for Stochastic Computations*. Princeton University Press, 2010.

[62] K. Yee. Numerical solution of inital boundary value problems involving maxwell's equations in isotropic media. *IEEE Trans. Antennas Propagat.*, 14(3):302–307, 1966.

[63] J. L. Young and R. O. Nelson. A summary and systematic analysis of FDTD algorithms for linearly dispersive media. *IEEE Antennas and Propagation Magazine*, 43:61–77, 2001.

[64] XM Zhong, C. Liao, W. Chen, ZB Yang, Y. Liao, and FB Meng. Image reconstruction of arbitrary cross section conducting cylinder using UWB pulse. *Journal of Electromagnetic Waves and Applications*, 21(1):25–34, 2007.